

Solving Random Satisfiability Problems with Quantum Computers

Tad Hogg
Xerox Palo Alto Research Center
Palo Alto, CA 94304
hogg@parc.xerox.com

November 6, 2018

Abstract

Quantum computer algorithms can exploit the structure of random satisfiability problems. This paper extends a previous empirical evaluation of such an algorithm and gives an approximate asymptotic analysis accounting for both the average and variation of amplitudes among search states with the same costs. The analysis predicts good performance, on average, for a variety of problems including those near a phase transition associated with a high concentration of hard cases. Based on empirical evaluation for small problems, modifying the algorithm in light of this analysis improves its performance. The algorithm improves on both GSAT, a commonly used conventional heuristic, and quantum algorithms ignoring problem structure.

1 Introduction

Peter Shor's polynomial-time factoring algorithm [47, 8] showed quantum computers [11, 12, 15, 50] efficiently solve an important problem thought to require exponential time on our current, "classical", machines. Can quantum computers significantly improve other apparently intractable problems? At first sight, combinatorial searches, such as arise in scheduling, theorem proving, cryptography, genetics and statistical physics, are one possibility. This is because many such searches are "non-deterministic polynomial" (NP) problems [18], which have a rapid test of whether a candidate solution is in fact a solution and an exponential growth in the number of candidates with the size of the problem. Quantum computers can test all candidates in superposition with about as many operations as a classical machine uses to test just one, suggesting large improvements are possible. Unfortunately, the difficulty of extracting a solution from the superposition appears to preclude rapid solution of at least some NP problems [2].

Nevertheless, quantum computers may offer substantial improvement for *typical* searches encountered in practice. For instance, constraint satisfaction problems [40] consist of constraints on the values various combinations of variables can take. A candidate solution for such problems can not only be evaluated in terms of *whether* it satisfies all the constraints, but also in terms of *how many* constraints it violates. This additional information is often a useful guide to finding solutions, providing the basis for conventional heuristic searches. Such heuristics are substantially better than simpler techniques ignoring problem structure. For heuristics consisting of repeated independent trials, Grover's amplitude amplification [22] gives a quadratic speedup with quantum computers [4],

the best possible improvement for quantum methods based only on the test of whether candidates are solutions [2].

Any possibility of greater speedup requires a quantum algorithm using additional problem properties. For some small or relatively easy problems such algorithms perform well [26, 49]. More generally, quantum methods readily exploit precise information on states' distances to a solution [23], but such information is not readily available for hard searches. Thus an important question is whether, and to what extent, quantum computers can exploit readily computed properties of hard search problems. In particular, can they perform significantly more efficiently than classical heuristic methods?

This paper discusses a previous structured quantum search algorithm [27], based on evaluating, in superposition, the number of conflicts in all search states. The paper extends empirical evaluation of the algorithm's behavior for a class of hard search problems and compares it to a version of amplitude amplification not requiring prior knowledge of the number of solutions [3]. Furthermore, the paper gives an approximate asymptotic performance analysis that includes variation among amplitudes associated with states with the same number of conflicts. Specifically, the next two sections describe a class of hard search problems and the form of the quantum algorithm. The remainder of the paper presents the extended asymptotic analysis and compares with actual behavior based on small problem sizes feasible to evaluate via simulation on conventional machines.

As a note on notation, to compare the growth rates of various functions we use [21] $f = O(g)$ to indicate that f grows no faster than g as a function of n when $n \rightarrow \infty$. Conversely, $f = \Omega(g)$ means f grows at least as fast as g , and $f = \Theta(g)$ means both functions grow at the same rate.

2 An Ensemble of Hard Satisfiability Problems

Heuristics are often too complicated to allow exact analytical evaluation of their performance. Instead, they are usually evaluated empirically on a sample of problems. Such a test requires a hard problem ensemble, i.e., a class of problem instances and associated probability distribution for their selection with a high concentration of hard cases. For practical use, instances of the ensemble should be computationally easy to generate. Since typical instances of NP problems are often much easier than worst case analyses suggest, defining such ensembles is not trivial. Fortunately, such ensembles exist for a variety of NP-complete search problems [7, 36, 29]. Significantly, problems from such ensembles, associated with abrupt "phase transitions" in behavior, are particularly difficult for a variety of heuristics, on average. They thus provide good test cases.

The k -satisfiability (k -SAT) problem provides one example. It consists of n Boolean variables and m clauses. A clause is a logical OR of k variables, each of which may be negated. A solution is an assignment, i.e., a value, true or false, for each variable, satisfying all the clauses. An assignment is said to conflict with any clause it doesn't satisfy. An example 2-SAT problem instance with 3 variables and 2 clauses is v_1 OR (NOT v_2) and v_2 OR v_3 , which has 4 solutions, e.g., $v_1 = \text{false}$, $v_2 = \text{false}$ and $v_3 = \text{true}$. For $k \geq 3$, k -SAT is NP-complete [18], i.e., is among the most difficult NP problems.

For assignments r and s , which can be viewed as bit-vectors of length n , let $d(r, s)$ be the Hamming distance between them, i.e., the number of variables they assign different values. Let $c(s)$ denote the number of the m clauses conflicting with s , which depends on the particular problem instance considered. The quantity $c(s)$ can also be thought of as the cost associated with the assignment, and those with zero cost are solutions.

The random k -SAT ensemble with given n and m consists of instances whose m clauses are selected uniformly at random. Specifically, for each clause, a set of k variables is selected randomly

from among the $\binom{n}{k}$ possibilities. Then each of the selected variables is negated with probability $1/2$ to produce the clause. Thus each of the m clauses is selected, with replacement, uniformly from among the $N_{\text{clauses}} = \binom{n}{k}2^k$ possible clauses. The difficulty of solving such randomly generated problems varies greatly from one instance to the next. This ensemble has a high concentration of hard instances when $\mu \equiv m/n$ is near a phase transition in search difficulty [7, 36, 29]. At this transition, the fraction of soluble instances drops abruptly from near 1 to near 0. For random 3-SAT this transition is at about $\mu = 4.25$, the value used for the results presented here as well as extensive prior studies of classical heuristics for SAT. For soluble problems near the transition, the number of solutions S is exponentially large but a tiny fraction of all states, i.e., $S/2^n$ is exponentially small.

3 The Algorithm

The quantum algorithm examined here [27] has the same general form as amplitude amplification [22] but with amplitude phase adjustments based on the state costs and the problem ensemble parameters, i.e., n , k and m for random k -SAT. Importantly, the algorithm does not require characteristics of the problem instance that are costly to compute, e.g., the number of solutions.

The overall algorithm consists of a series of trials, each operating with superpositions of all 2^n assignments. Superpositions correspond to vectors with an amplitude for each assignment. After each trial, a measurement produces a single assignment. Trials repeat until a solution is found. Quantum coherence need persist only for the duration of each trial, rather than over all trials. For the case considered here, this duration grows linearly with n thereby placing less stringent coherence requirements on the hardware than amplitude amplification whose trial duration grows exponentially with n for hard problems (because, for hard problems, the number of solutions is an exponentially small fraction of the total number of states).

A trial performs a series of j steps. Each step evaluates the costs associated with all assignments and mixes amplitudes among them based on their Hamming distances. Starting with an equal superposition of all 2^n assignments, i.e., $\psi_s^{(0)} = 2^{-n/2}$, the superposition vector $\psi^{(j)}$ after j steps is

$$\psi^{(j)} = U^{(j)} P^{(j)} \dots U^{(1)} P^{(1)} \psi^{(0)} \quad (1)$$

The algorithm involves two types of matrices: the diagonal phase adjustments $P^{(h)}$, depending on the particular problem instance, and the matrix $U^{(h)}$, mixing amplitudes among states without regard to the particular instance.

Specifically, $P^{(h)}$ is diagonal with $P_{ss}^{(h)} = e^{i\pi\rho(h,c(s))}$ where $c(s)$ is the number of conflicts in assignment s and ρ is an arbitrary computationally-efficient real-valued function. Since $c(s)$ itself is efficiently evaluated (by comparing the state with each of the m clauses) and has only $m+1 = \Theta(n)$ possible values, $0, \dots, m$, quantum computers efficiently implement this matrix operation [30] as a generalization of the technique used for amplitude amplification.

Viewing assignments as strings of n bits, let W be the Walsh-transform, $W_{rs} = 2^{-n/2}(-1)^{|r \wedge s|}$ where $|r \wedge s|$ is the number of 1's the two assignments have in common. We define the mixing matrix as $U^{(h)} = WT^{(h)}W$ where $T^{(h)}$ is diagonal with $T_{ss}^{(h)} = e^{i\pi\tau(h,|s|)}$, $|s|$ denotes the number of 1-bits in s and τ is another computationally-efficient real-valued function. With these definitions, $U_{rs}^{(h)}$ depends only on the distance $d(r,s)$ [27], i.e., has the form $U_{rs}^{(h)} = u_{d(r,s)}^{(h)}$. Quantum computers evaluate this matrix operation efficiently [22, 3, 30].

Observing the final superposition gives an assignment having c conflicts with probability

$$p^{(j)}(c) = \sum_{s|c(s)=c} |\psi_s^{(j)}|^2$$

with the sum over all assignments with c conflicts. In particular, $P_{\text{soln}}(j) = p^{(j)}(0)$ is the probability to find a solution in a single trial.

Completing the algorithm requires specifying functional forms for the phase adjustment functions ρ and τ . Since $c(s)$ and $|s|$ are integers, the matrix elements are unchanged by adding any multiple of 2 to either ρ or τ . Moreover, changing the sign of both values simply conjugates the matrix elements. Thus, without loss of generality, we can restrict the ρ values to be in the range $(-1, 1]$ and τ in $[0, 1]$. In the remainder of this section we describe the special case equivalent to amplitude amplification and then discuss one way to include problem structure.

3.1 Amplitude Amplification

In the notation introduced above, amplitude amplification consists of the choices

$$\begin{aligned}\rho(h, c) &= \begin{cases} 1 & \text{if } c = 0 \\ 0 & \text{otherwise} \end{cases} \\ \tau(h, b) &= \begin{cases} 1 & \text{if } b = 0 \\ 0 & \text{otherwise} \end{cases}\end{aligned}$$

These choices, which are the same for all steps (i.e., independent of h), cause P to invert the amplitude of solutions and make U a diffusion matrix with $u_d = -\delta_{d0} + 2^{1-n}$ where δ_{ab} is one if $a = b$ and zero otherwise. Note the off-diagonal elements of U are exponentially small.

By treating all nonsolution states equally, this algorithm has the major advantage of a simple expression for the probability to find a solution after j steps, namely [3]

$$P_{\text{soln}}(j) = \sin((2j + 1)\theta)^2 \tag{2}$$

where $\theta = \sin^{-1} \sqrt{S/2^n}$ and S is the number of solutions. For hard, soluble random k -SAT, $2^n \gg S \gg 1$ and $\theta \sim \sqrt{S/2^n}$ is exponentially small. Thus the algorithm can give $P_{\text{soln}} = \Theta(1)$ when $j = \Omega(1/\theta)$, i.e., after an exponentially large number of steps for hard problems.

In practice, S is not known a priori, so the best choice for the number of steps j cannot be determined. A useful alternative selects j differently for each trial as follows [3]: Starting with $M = 1$,

- perform a single amplitude amplification trial with the number of steps j selected randomly between 0 and $M - 1$
- if a solution is found, stop. Otherwise, set $M = \min(2^{n/2}, 6M/5)$ and repeat.

This procedure increases the expected cost, compared to having prior knowledge of S , by at most a factor of 4 [3]. For the sake of definite comparison with other choices for ρ and τ , we describe how to evaluate the expected number of steps to find a solution.

In light of Eq. 2, selecting the number of steps j uniformly at random between 0 and $M - 1$, gives the probability to obtain a solution [3]

$$p_{\text{random}}(M) = \frac{1}{M} \sum_{j=0}^{M-1} P_{\text{soln}}(j) = \frac{1}{2} - \frac{\sin(4M\theta)}{4M \sin(2\theta)} \tag{3}$$

which approaches 1/2 as M increases.

The trial with a given M takes $(M - 1)/2$ steps, on average. With probability $1 - p_{\text{random}}(M)$ the trial is not successful. Thus the expected cost for all trials starting with M is

$$\text{cost}(M) = \frac{M - 1}{2} + (1 - p_{\text{random}}(M)) \text{cost}(\min(2^{n/2}, 6M/5)) \quad (4)$$

When $M \geq 2^{n/2}$, further iterations have $M = 2^{n/2}$ so Eq. 4 gives

$$\text{cost}(2^{n/2}) = \frac{2^{n/2} - 1}{2 p_{\text{random}}(2^{n/2})}$$

For hard, soluble random k -SAT, $p_{\text{random}}(2^{n/2}) \sim 1/2$ so $\text{cost}(2^{n/2}) \sim 2^{n/2}$. This condition and Eq. 4 allow computing the expected cost of the entire loop, i.e., $\text{cost}(1)$, recursively.

3.2 Using Problem Structure

With the algorithm described here, using problem structure is conceptually straightforward: for a class of problems, such as random k -SAT with given n and m , select values for the phase functions $\rho(h, c)$ and $\tau(h, b)$ to minimize the search cost for typical instances of the class. We take the number of steps in each trial, j , to grow only polynomially with n . Furthermore, $m = \Theta(n)$ for hard random k -SAT. Thus the number of values to specify ρ and τ grows polynomially with n . In particular, for j growing linearly with n , $\Theta(n^2)$ values completely specify these functions.

We thus have a situation commonly found with developing conventional heuristics: a number of algorithm parameters to tune with respect to the class of problems. Generally, the heuristics are too complicated to permit a useful analytical relation between the parameter values and algorithm cost. Instead, one takes a sample of problem instances and solves them with various choices for the parameter values. Numerical optimization techniques can then find parameter values giving good performance for the sample, e.g., minimizing the median search cost for the sample. These values are evaluated by using them to solve another sample drawn from the same problem ensemble. Since the cost of these heuristics grows exponentially for hard problems, this sampling technique is limited to relatively small problems. Nevertheless, efficient implementations often allow investigating SAT problems with hundreds or thousands of variables.

These remarks also apply to heuristics for quantum computers. On a quantum machine, each trial requires only polynomial time. On the other hand, at least for most parameter choices, P_{soln} is exponentially small, thus requiring exponentially many trials to estimate P_{soln} on the sample's problem instances. Hence a direct attempt to find parameter values minimizing the median search cost would require exponentially many trials. One way to address this difficulty is to identify how good parameter choices scale with n and then perform the parameter value optimization with smaller n . An example of such scaling is having the phase parameters scale as $1/j$, as described below. Another approach makes use of the shift in amplitudes toward low-cost states, illustrated in §4. Thus, instead of maximizing P_{soln} , we could minimize the expected cost of the state produced by a trial, a quantity easily estimated with a modest number of trials.

Currently, however, such quantum machines do not exist. Instead, we must simulate the quantum algorithm on conventional machines, so each trial requires exponential cost and memory. Thus we are limited to investigating much smaller problems, up to 20 variables or so for SAT. In particular, the simulation evaluates properties of all search states and so is considerably more expensive than evaluating conventional heuristics. The latter, while having exponentially growing costs, typically evaluate only a tiny portion of the full search space.

The number of function evaluations for a numerical optimization procedure grows with the number of values to optimize. Thus as a practical matter, we consider only a restricted set of

possible values with a smaller number of independent parameters. In particular, a study of this algorithm with a fixed number of steps [28] suggests restricting ρ and τ to vary linearly with the number of conflicts c and number of 1-bits b , respectively, only slightly reduces the performance. We make this restriction in the specific form for the heuristic presented below.

An alternate approach to finding good parameter values, also discussed below, uses an approximate analytical theory of the algorithm performance. The theory allows rapid evaluation of the approximate performance for a given choice of parameter values. We can then apply numerical optimization to find values giving high performance according to this approximation. This approach allows evaluating behavior for much larger problem sizes, but with the caveat of being only an approximation.

3.3 Parameter Choices to Use Problem Structure

To exploit problem structure, we introduce two real-valued functions $R(\lambda)$ and $T(\lambda)$ defined over $0 \leq \lambda \leq 1$. These functions specify the amplitude adjustments made, respectively, by the cost evaluation and mixing, as a function of the number of steps completed. Specifically, R and T define the phase adjustment functions as

$$\begin{aligned}\rho(h, c) &= \rho_h c \\ \tau(h, b) &= \tau_h b\end{aligned}$$

with

$$\begin{aligned}\rho_h &= \frac{1}{j} R\left(\frac{h-1}{j}\right) \\ \tau_h &= \frac{1}{j} T\left(\frac{h-1}{j}\right)\end{aligned}\tag{5}$$

for steps $h = 1, \dots, j$. These values decrease as $1/j$ so P and U are close to identity matrices as j increases. When iterated over the j steps of a trial, these operations nevertheless substantially shift amplitudes among the assignments. The linearity of $\tau(h, b)$ with respect to b means the elements of the mixing matrix are [27]:

$$u_d^{(h)} = \left(e^{i\pi\tau_h/2} \cos\left(\frac{\pi\tau_h}{2}\right) \right)^n \left(-i \tan\left(\frac{\pi\tau_h}{2}\right) \right)^d\tag{6}$$

Thus the elements decrease rapidly with d so the largest mixing is among states close to each other. In the case we consider, j grows as a power of n (allowing individual trials to complete in polynomial time). This means the off-diagonal terms of U corresponding to $d = O(1)$ decrease as a power of n rather than the exponential decrease of the diffusion mixing matrix.

Completing the algorithm requires explicit forms for $R(\lambda)$ and $T(\lambda)$ and the number of steps j . Ideally these quantities would minimize the expected total number of steps in all trials for the particular problem instance. For hard problems, such optimal choices are not known a priori. Thus we focus instead on functional forms giving good performance on average for random k -SAT, i.e., depending only on the ensemble parameters n , k and m . While the values could vary from one trial to the next, in analogy with the procedure described above for amplitude amplification when the number of solutions is not known, for simplicity we use the same values for each trial. The expected cost to find a solution is then j/P_{soln} . While such choices will not be optimal for each instance, they can nevertheless improve average performance, as shown below.

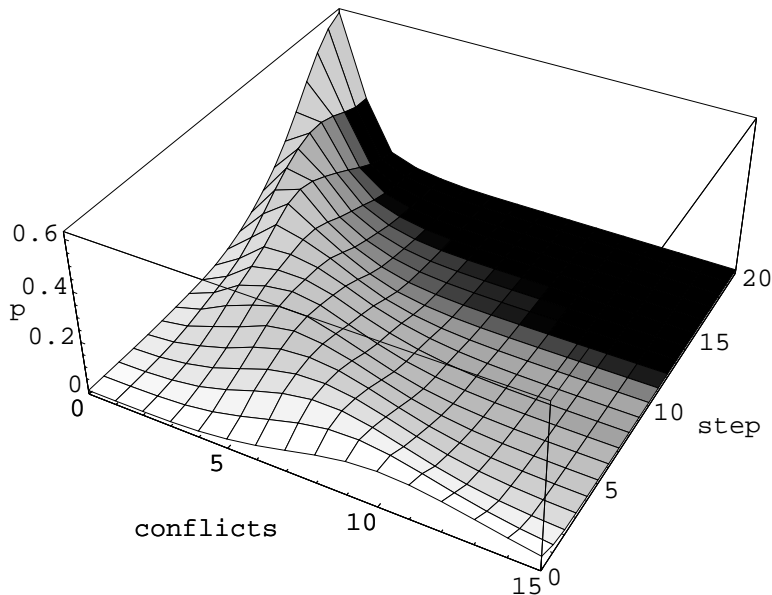


Figure 1: Solving a randomly generated 3-SAT problem with $n = 20$ and $\mu = 4.25$. For each step h , the figure shows the probability $p^{(h)}(c)$ in assignments with each number of conflicts. Shading is based on the relative deviations of the amplitudes, described in the text. The small contributions for assignments with $c > 15$ are not included. This instance has 20 solutions.

4 Algorithm Behavior

This section illustrates the algorithm's behavior for small problems, and compares it to amplitude amplification. These observations motivate the approximate analyses of the following section.

For $\mu = 4.25$, using $j = n$ and linear forms for R and T gives reasonably good performance. Specifically [27], for

$$\begin{aligned} R(\lambda) &= R_0 + R_1(1 - \lambda) \\ T(\lambda) &= T_0 + T_1(1 - \lambda) \end{aligned} \tag{7}$$

with $R_0 = 4.86376$, $R_1 = -4.18118$, $T_0 = 1.2$ and $T_1 = 3.1$, Fig. 1 shows the behavior for one problem instance. These numerical values were determined from the approximate analysis, based on average amplitudes, discussed in §5.2.

This figure illustrates several properties of the algorithm. First, at each step, probability is concentrated in states with a fairly small range of costs. Each step shifts the peak in the probability distribution toward assignments with fewer conflicts, until a large probability builds up in the solutions. This shift is also seen for other problem instances (with differing final probabilities) and when averaged over many samples. The peaks become sharper for larger n , with relative widths decreasing as $O(1/\sqrt{n})$. By contrast, amplitude amplification increases the probability in solutions but all other amplitudes decrease uniformly.

Second, the variation of amplitudes among states with the same cost is relatively large only in the last few steps of the algorithm and then primarily for higher-cost states for which the amplitudes are small. The shading in Fig. 1 shows this behavior, indicating the relative deviation of the amplitudes

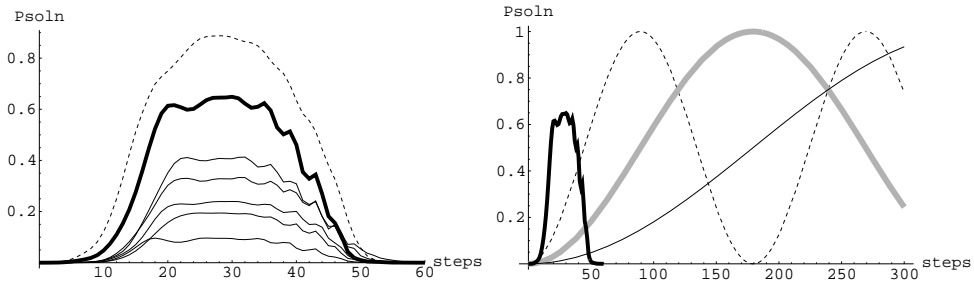


Figure 2: P_{soln} as a function of the number of steps for several 3-SAT instances. The first plot shows the behavior of the heuristic algorithm with the same parameters as Fig. 1 and using $j = n$ to define the phase parameters in Eq. 5. The dashed curve is an instance with 80 solutions, the thick solid curve is the instance with 20 solutions of Fig. 1 and the thin solid curves are different instances with 5 solutions. The second plot shows the behavior of amplitude amplification with 80, 20 and 5 solutions for the dashed, gray and solid curves, respectively. For comparison, the 20-solution curve from the first plot is also included.

(i.e., ratio of standard deviation to mean) for states with the each cost, ranging from white for zero deviation to black for relative deviations greater than 3.

Fig. 2 gives further insight into the algorithm. Unlike amplitude amplification, the heuristic reaches its maximum P_{soln} at about the same number of steps for problems with differing numbers of solutions. Instead, the variation is in the maximum value of P_{soln} . Even instances with the same number of solutions behave differently. Thus for this algorithm, identifying the appropriate number of steps is not an issue, rather the difficulty is in selecting appropriate phase parameter adjustments. As problem size increases, the number of steps required for amplitude amplification increases exponentially and always gives $P_{\text{soln}} \approx 1$. By contrast, the heuristic uses a linearly growing number of steps but P_{soln} gets small.

To compare the net effect of these contrasting behaviors, we examine the search cost scaling of the two methods. Using the parameters of Eq. 7, Fig. 3 shows the growth of the expected search cost for randomly generated problems, i.e., the expected number of steps, $j/P_{\text{soln}}(j)$. The exponential fit gives the cost growing as $e^{0.10n}$. As one caveat, we should note most of the P_{soln} values are fairly large for these problem sizes, i.e., $P_{\text{soln}} \geq 0.3$, thus usually finding a solution after only a few trials. Thus much of the variation in costs shown here is due to the linear growth of the number of steps j , and it may require larger problems to see the cost growth dominated by the behavior of P_{soln} .

Fig. 4 shows another property of the heuristic: as long as j/n is not too small, P_{soln} does not change much as j increases. This can be understood from the scaling of phase parameters of Eq. 5. When $j \gg 1$, the algorithm matrices are close to the identity. In this situation, when j is doubled, the phase adjustments are halved so two steps change the amplitudes about as much as the original choice of j did in one step. As a further observation, the minimum median cost, $j/\text{median}(P_{\text{soln}})$, occurs at somewhat smaller ratios of j/n as n increases. Exploiting this decrease gives somewhat lower costs for the quantum heuristic than those shown in Fig. 3, which used $j/n = 1$. As a further observation, the value of j/n giving about half the maximum P_{soln} for each n decreases close to linearly on a log-log plot with a slope of about -0.8, indicating the best scaling performance requires only $j = O(n^{0.2})$. If this behavior continues to hold for larger n , the approximate analysis discussed below, based on $j \gg \sqrt{n}$, would somewhat overestimate the minimum possible costs.

Finally we should note the distinction between Fig. 2 and Fig. 4. In the former, the phase parameters of Eq. 5 are defined using $j = n$ and the behavior of P_{soln} is shown for trials of various

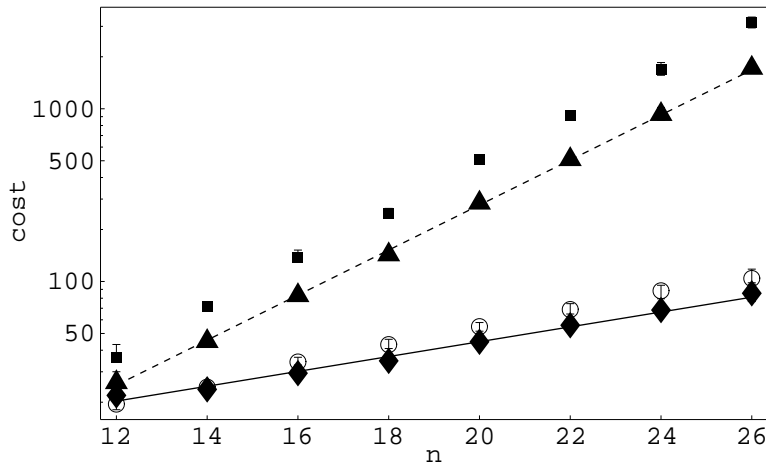


Figure 3: Log-plot of median search cost vs. n for the quantum heuristic (diamond), amplitude amplification (assuming the number of solutions is known (triangle) or not (square)), and GSAT [45] with restarts after $2n$ steps (circle). For each n , the same 1000 soluble random 3-SAT problems with $\mu = 4.25$ were solved with each method (except only 500 and 400 samples for $n = 24$ and 26 , respectively). For those n not divisible by 4, half the samples had $m = \lfloor 4.25n \rfloor$ and half had m larger by one. Error bars show the 95% confidence intervals [48, p. 124], which in many cases are smaller than the plotted point. The curves show exponential fits to the quantum heuristic (solid) and amplitude amplification (dashed).

numbers of steps using these fixed parameters. In the latter figure, j varies and gives different phase parameters at each value of j/n , and P_{soln} is shown after completing j steps.

4.1 Comparing with Amplitude Amplification

Provided the number of solutions S is known, the cost for amplitude amplification is [3] $\frac{\pi}{4}\sqrt{2^n/S}$, also shown in Fig. 3. The values grow as $e^{0.30n}$, i.e., about three times faster than the quantum heuristic.

In practice, S is not known a priori, requiring the modified algorithm, described in §3.1, whose expected cost is less than four times larger [3], so does not affect the exponential growth rate. However, for the sake of a definite comparison with the quantum heuristic, which also does not use prior knowledge of the number of solutions, we compute the actual expected cost of the modified algorithm using Eq. 4. The resulting values, included in Fig. 3, are slightly less than twice as large as the cost for amplitude amplification when S is known.

4.2 Comparing with a Conventional Heuristic

Average costs for even the best known classical heuristics grow exponentially. For instance, Fig. 3 shows the search cost for a good classical heuristic, GSAT [45], grows slightly faster than this quantum heuristic. The GSAT algorithm starts from a random assignment and, for each step, examines the number of conflicts in the assignment’s neighbors (i.e., assignments obtained by changing the value for a single variable) and moves to a neighbor with the fewest conflicts. If a solution isn’t found after a prespecified number of steps, e.g., because the current assignment is a local minimum, the search is tried again from a new random assignment. The most significant comparison between

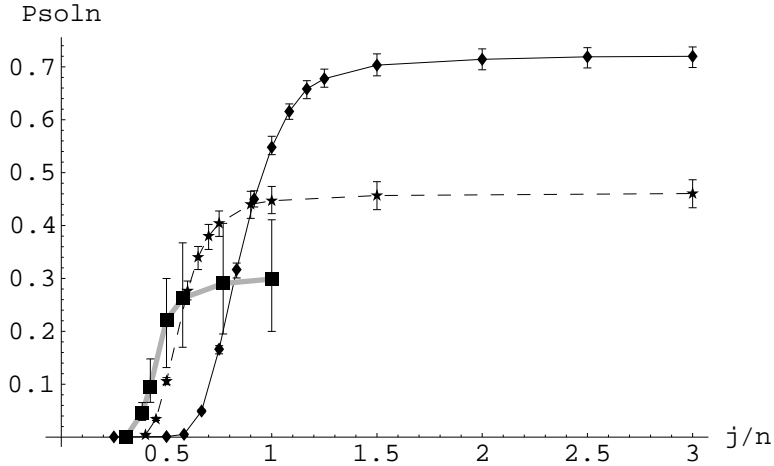


Figure 4: Median solution probability vs. j/n for the quantum heuristic for 1000 random 3-SAT problems with $n = 12$ (solid) and $n = 20$ (dashed), and 60 samples with $n = 26$ (gray). For these cases $\mu = 4.25$. Error bars show the 95% confidence intervals.

GSAT and the quantum heuristic is the relative growth rates in the search costs, as measured by the number of steps. The corresponding actual search times will depend on detailed implementations of the steps. Although the number of elementary computational steps, involving evaluating the number of conflicts in an assignment (and, in the case of GSAT, its neighbors) are similar for both techniques, differences in the extent to which operations can be optimized away (e.g., as is possible in some cases for NMR-based quantum implementations [10]) and the relative clock rates of classical and quantum machines remain to be seen.

At any rate, the figure shows that including the number of conflicts in the phase adjustments reduces the number of steps required for the quantum algorithm below that required for GSAT, on average. Because the trials are independent, both the quantum heuristic introduced here and GSAT can be quadratically improved with amplitude amplification [4], amounting to decreasing the growth rates shown in the figure by a factor of two. Such an improvement requires extending coherence across multiple trials, rather than just a single one.

This technique also generalizes to allow the quantum heuristic presented here to work with the results of deterministic classical heuristics with independent trials (e.g., a deterministic version of GSAT in which, say, any ties are broken by selecting the first neighbor with minimum cost in a lexicographic ordering of the states, or the seed used with the random number generator is prespecified for all trials). Specifically, instead of basing the phase adjustment on the number of conflicts in a state, we run GSAT starting from that state for a fixed number of steps. We can then use the number of conflicts of the resulting state as the basis for the phase adjustment. This thus uses more information about the heuristic than just combining it with amplitude amplification, which tests whether the heuristic finds a solution [4]. For the problem sizes discussed here, using this technique gives considerably higher probabilities to find a solution, even using the same phase adjustment parameters as used for the original method involving the number of conflicts in the states. However, the additional steps required to evaluate GSAT within each trial, results in a larger overall cost. Nevertheless, this technique may be useful for larger problem sizes, where the probabilities to find solutions are lower.

From this discussion, the structured quantum algorithm appears to improve on GSAT for hard SAT problems, but definitive statements cannot be made based only on such small problems. Unfortunately, classical simulations of quantum machines incur an exponential growth in time and memory, preventing evaluation with larger problems. More extensive empirical evaluation requires either faster simulation techniques, perhaps approximate [5], or quantum computers.

5 Approximate Analyses of Behavior

The usual approach to evaluating conventional heuristics, and tuning any adjustable parameters they may have, is by running them on a sample of problems. This is necessary because analytical methods are often unable to account for the complicated dependencies in the search path explored by the heuristic. As discussed in the previous section, such simulations are also useful for quantum algorithms, but are limited to small problems.

As a complementary approach, we consider approximate analytical techniques. The average properties of random k -SAT successfully help understand and improve search methods, both classical [13, 7, 24, 19] and quantum [27]. In particular, the quantum algorithm operates with the entire search space at each step so its performance depends on averaged properties of the search states. For simple ensembles, such as random k -SAT, such averages are readily computable and thus give asymptotic characterizations of the problems for large n . In addition to estimating algorithm performance, such analyses provide insight into the qualitative features of the behavior seen empirically.

For a problem instance P , let $\psi_s^{(h)}(P)$ be the amplitude for state s after completing step h of the algorithm. Initially, $\psi_s^{(0)}(P) = 2^{-n/2}$. A single step of the algorithm, from Eq. 1, gives

$$\psi_r^{(h)}(P) = \sum_s u_{d(r,s)}^{(h)} e^{i\pi\rho_h c(s)} \psi_s^{(h-1)}(P) \quad (8)$$

The remainder of this section discusses techniques using the properties of random k -SAT to estimate the algorithm's behavior for large n , and suggest suitable choices for the phase functions.

5.1 Average P_{soln}

Ideally, we would like to estimate the typical search cost for problems in the ensemble. The expected cost for a given problem instance is j/P_{soln} . Thus one quantity to examine is the ensemble-average $\langle j/P_{\text{soln}} \rangle$ or, since, in the case considered here, j is the same for all instances, $j\langle 1/P_{\text{soln}} \rangle$. However, this quantity is infinite if even a single problem instance is insoluble. Even restricting attention to soluble instances, we find a wide variation in solution costs. Thus the average is dominated by a small fraction of the instances and does not indicate typical behavior. A better indication is the median value of j/P_{soln} , but is difficult to treat analytically. As an analytically tractable quantity, we focus instead on $j/\langle P_{\text{soln}} \rangle$.

The random k -SAT ensemble includes both soluble and insoluble instances, so $\langle P_{\text{soln}} \rangle \leq P_{\text{soluble}}$, the fraction of soluble instances in the ensemble. Below the phase transition, near $\mu = 4.25$ for random 3-SAT, $P_{\text{soluble}} \rightarrow 1$. For larger μ , $P_{\text{soluble}} \rightarrow 0$ as n increases, in which case the performance for *soluble* problems is given instead by $\langle P_{\text{soln}} \rangle / P_{\text{soluble}}$. Unfortunately, the random k -SAT ensemble does not have a simple expression for P_{soluble} , or even just its leading exponential scaling rate, precluding an exact evaluation for overconstrained soluble problems. One approach to estimate this behavior uses empirical classical search to evaluate P_{soluble} for a range of problem sizes for a given value of μ . The behavior of these values as a function of n then estimates the scaling of P_{soluble} .

For instance, samples of 10^4 problems for n from 50 to 250 show [44] close to exponential decrease of P_{soluble} for μ values somewhat above the transition. The resulting estimates of the actual decay rates for P_{soluble} are 0.011, 0.025 and 0.045 for μ equal to 4.5, 4.7 and 4.9, respectively. Analytic bounds on the behavior of P_{soluble} for μ between 4.2 and 5.2 are difficult to obtain. One such result is $P_{\text{soluble}} \leq \exp(-5.9 \times 10^{-5}n)$ at $\mu = 4.762$ [33], which is a considerably smaller decay rate than suggested by empirical evaluation. Above $\mu = 5.2$, the expected number of solutions, $\langle S \rangle$, goes to zero, so the Markov bound $P_{\text{soluble}} \leq \langle S \rangle$ provides another constraint.

For random k -SAT $\langle P_{\text{soln}} \rangle$ is

$$\frac{1}{N_{\text{clauses}}^m} \sum_P \sum_{s|c(s)=0} |\psi_s^{(j)}(P)|^2 \quad (9)$$

where the outer sum is over the N_{clauses}^m possible problem instances and the inner sum is over those assignments s that are solutions for P . Since the clauses are selected independently, the sum over problems is equivalent to m sums, each of which ranges over N_{clauses} possible clauses. Interchanging the order of summation gives an outer sum over all assignments s and an inner sum over those problem instances for which s is a solution, i.e., instances containing no clause conflicting with s . Since the random k -SAT ensemble treats all assignments equally, this sum over problems is the same for all choices of s . Thus we can focus on a single assignment, say $s = 0 \dots 0$. For an assignment r and clause σ , let $\alpha(r, \sigma) = 1$ if σ conflicts with r and otherwise is zero. Then $c(r)$ for problem instance P is the sum of $\alpha(r, \sigma)$ over the clauses in P . With this notation, Eq. 1 gives $\langle P_{\text{soln}} \rangle$ equal to

$$\sum_{\substack{s_0, \dots, s_{j-1} \\ s'_0, \dots, s'_{j-1}}} \left(\prod_{h=1}^j v_h v_h'^* \right) \left(\frac{1}{N_{\text{clauses}}} \sum_{\sigma} \exp \left(i\pi \sum_h \rho_h (\alpha_h - \alpha'_h) \right) \right)^m \quad (10)$$

where $v_h \equiv u_{d(s_h, s_{h-1})}^{(h)}$, $v'_h \equiv u_{d(s'_h, s'_{h-1})}^{(h)}$, $\alpha_h \equiv \alpha(s_{h-1}, \sigma)$, $\alpha'_h \equiv \alpha(s'_{h-1}, \sigma)$ and we define $s_j \equiv s'_j \equiv s$. The σ sum is over all clauses not conflicting with $s = 0 \dots 0$, i.e., those σ with $\alpha(s, \sigma) = 0$.

For constant j , an exact asymptotic analysis [28] shows $\langle P_{\text{soln}} \rangle$ decays exponentially but at smaller rates than the exponential growth in number of steps required by amplitude amplification. Fig. 5 shows examples for j up to 5: specifically the decay rate A defined by $\langle P_{\text{soln}} \rangle \sim \exp(-An)$. For example, with $\mu = 4.25$, for $j = 5$ the decay rate is $A = 0.13$, only slightly larger than the empirical growth rate of the median cost shown in Fig. 3 when $j = n$. This may indicate the problem sizes feasible to simulate are not large enough to show the full benefit of allowing j to grow with n .

This analysis is useful in suggesting the scaling behavior of Eq. 5 for the algorithm's parameters and shows $\langle P_{\text{soln}} \rangle$ decreases less rapidly as j increases. Unfortunately, this analysis is not applicable to the more interesting situation where the number of steps j grows with n . While it may be possible to develop approximations for $j \gg 1$, a simpler approach uses the observed properties of the amplitudes seen in §4. This approach is described in the remainder of this section.

5.2 Average Amplitudes

Empirical evaluations show that amplitudes for states with the same number of conflicts are generally quite similar. This observation motivates an analysis based on the behavior of the average amplitude for states with each cost [27]. Consider the quantity $A_C^{(h)}$ defined as $\langle \psi_s^{(h)}(P) \rangle$ with the average first over all states s with $c(s) = C$ in the problem instance P , and then over all problems in the

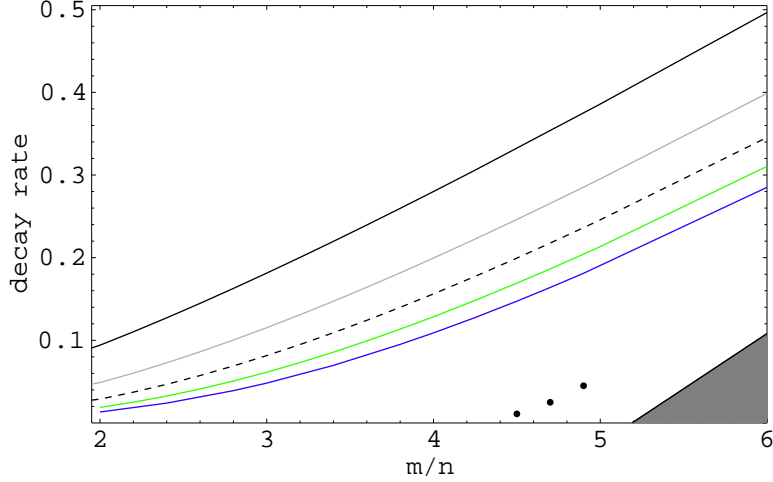


Figure 5: Minimum decay rates for $\langle P_{\text{soln}} \rangle$ as a function of $\mu = m/n$ (from top to bottom) $j = 1$ through 5 steps using linear variation in phase parameters with step number (i.e., of the form given in Eq. 7), but with different numerical values for each j . The points indicate empirical estimates of the decay rate for P_{soluble} , a lower bound on the decay rate for P_{soln} . The upper edge of the filled region is, in turn, a lower limit on P_{soluble} given by the Markov bound using the expected number of solutions.

random k -SAT ensemble with given n and m . Assuming amplitudes for states with the same cost are the same, at least for the dominant cost states at each step, Eq. 8 becomes

$$A_C^{(h)} \approx \sum_{d,c} u_d^{(h)} e^{i\pi\rho_h c} v_d(C,c) A_c^{(h-1)} \quad (11)$$

where $v_d(C,c)$ is the expected number of states with c conflicts at distance d from a state with C conflicts. Significantly, $v_d(C,c)$ is a property of the problem ensemble, independent of the algorithm details. For random k -SAT, $v_d(C,c)$ is a multinomial sum described briefly in the appendix.

Simulations show probability concentrates in a small range of cost values, as illustrated schematically in Fig. 6. These dominant costs are, in turn, close to the average cost $\sum_C C v(C) |A_C|^2$ where $v(C)$ is the expected value, for random k -SAT, of the number of states with C conflicts. We can thus expand $A_c \approx A_C Z^{c-C}$, around the average cost, with Z a complex number depending on the step.

In one step, Eq. 11 implies Z changes by $O(1/j)$. So for $j \gg 1$, Z becomes a smooth function of $\lambda = h/j$ satisfying the differential equation [27]

$$Z_\lambda = i\pi Z \left(R - \frac{T}{2} k f \frac{(1-p(1-Z))(1-Z)}{(1-p)Z} \right) \quad (12)$$

where $\chi = \frac{|Z|^2 p}{1-p(1-|Z|^2)}$ and

$$f = \exp \left(-k\mu(1-Z) \left(\frac{p(1-\chi)}{1-p} - \frac{\chi}{Z} \right) \right)$$

The initial condition, corresponding to all amplitudes equal, is $Z(0) = 1$. With this approximation, the dominant cost value is χm .

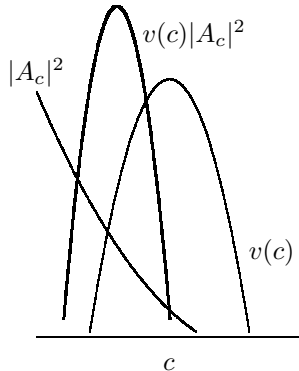


Figure 6: Schematic behavior of average amplitudes, on a logarithmic scale, as a function of number of conflicts c . The average number of states with c conflicts, $v(c)$, is sharply peaked around the average number of conflicts $m/2^k$. When the magnitude of the amplitudes decreases rapidly with c , as shown here, the probability in states with c conflicts is also sharply peaked, but at a somewhat lower value, corresponding to the shift seen in Fig. 1. Quantitatively, the values decrease exponentially with n , so the logarithms, shown here, are proportional to n and the relative width of each peak is $O(1/\sqrt{n})$.

With suitable choices for R and T , such as those in Eq. 7 for $k = 3, \mu = 4.25$, Eq. 12 gives $Z(1) = 0$ thereby predicting most of the amplitude concentrates in states with the fewest conflicts, i.e., solutions if the problem instance is soluble.

5.3 Including Variation Among Amplitudes

The approximation based on average amplitudes shows good correspondence with empirical evaluation for most of the steps of the algorithm. However the variation among amplitudes with the same costs increases for the last few steps of the algorithm, as illustrated in Fig. 1. If this variation remains significant as problem sizes increase, especially among states with fairly low costs, it remains possible that the small averages predicted for nonsolution states when $Z(1) = 0$ are due to large variation in the phases of the amplitudes rather than small magnitudes, leading to somewhat less concentration in solution states than predicted.

It is thus useful to estimate the contribution from this variation to the behavior of the algorithm. A direct approach would consider the ensemble-average of the variance in amplitudes among states with each cost. Such an analysis gives a similar prediction, namely appropriate phase functions can concentrate amplitude sufficiently into low-cost states to give high average performance. To avoid introducing significant variation in amplitudes for states with the same cost, the resulting phase adjustments are smaller than those based on the behavior of the average amplitudes alone. Using such parameters for small problems gives significantly lower P_{soln} values, and hence higher costs, than shown in Fig. 3. Since the analysis assumes $\sqrt{n} \gg 1$, this poor performance for small n could be due to the small problem sizes.

Another possibility is the analysis based on the variance of amplitudes overestimates the effect of amplitude variation. Specifically, in the case treated here, where the number of steps grows with n , most contribution to the amplitude of a given state is from other states relatively near to it. This is due to the decreasing values of τ_h in Eq. 5 causing the mixing matrix elements u_d in Eq. 6 to

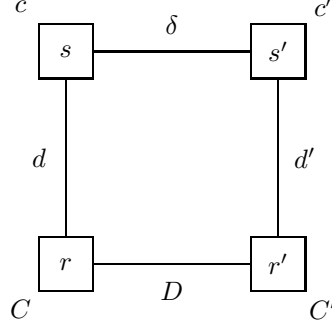


Figure 7: Distance relations and costs for the four assignments r, r', s and s' .

decrease rapidly with distance. Thus large variations among amplitudes for states that are far apart do not much affect the result of a single step. Conversely, nearby states share many of the same neighbors so their amplitudes are likely to be more correlated than those of distant states. This means a useful characterization of the amplitude variations should also account for the distance between the states. Thus we consider an approximation based on the assumption that *nearby* states with the same costs have approximately the same amplitudes.

Consider the quantity $S_{D,C,C'}^{(h)}$ defined as $\langle \psi_s^{(h)}(P) \psi_{s'}^{(h)}(P) \rangle$ with the average first over all pairs of states s, s' such that $d(s, s') = D$ and $c(s) = C, c(s') = C'$ in the problem instance P , and then over all problems in the random k -SAT ensemble with given n and m . A mean-field approximation with Eq. 8 gives

$$S_{D,C,C'}^{(h)} \approx \sum_{d,d',\delta,c,c'} u_d^{(h)} u_{d'}^{(h)*} e^{i\pi\rho_h(c-c')} v_{D,d,d',\delta}(C, C', c, c') S_{\delta,c,c'}^{(h-1)} \quad (13)$$

where $v_{D,d,d',\delta}(C, C', c, c')$ is the ensemble average of the number of assignment pairs s, s' with costs c, c' , respectively, with distance relations $d(s, s') = \delta, d(r, s) = d, d(r', s') = d$, averaged over all assignment pairs r, r' with $d(r, r') = D$ and costs C, C' , respectively, as illustrated in Fig. 7.

Eq. 13 uses $v_{D,d,d',\delta}(C, C', c, c')$, which characterizes the relevant structure of the problems and is independent of the search algorithm choices for $R(\lambda)$ and $T(\lambda)$. As with $v_d(C, c)$, this 4-state structure quantity is a sum of products of multinomials. As described in the appendix, an expansion similar to that described above for the average amplitude A_C gives an asymptotic expansion of Eq. 13 for large problem sizes. Specifically, we express the behavior for S with the expansion near $D = 0, c \approx C, d \approx D$ of $S \propto Y^d X^c$, with $X \equiv r e^{i\theta}$ and Y depending on the step. For $j \gg 1$, these values change slowly from one step to the next giving differential equations:

$$\begin{aligned} Y_\lambda &= \pi T \left(Y^2 k \mu F \frac{\nu}{1-p} (1-r) (1+p(-1+kr)) \sin(\theta) + G \sin(B) \right) \\ r_\lambda &= -\frac{\pi T}{2} k Y F \frac{\nu}{1-p} \sin(\theta) \\ \theta_\lambda &= \pi R - \frac{\pi T}{2r} \left(G \frac{1}{Y} (\cos(B-\theta) - r^2 \cos(B+\theta)) - F Y (k-1)(r - \cos(\theta)) \right) \end{aligned} \quad (14)$$

with

$$F = \exp(-\nu k \mu (1 + r^2 - 2r \cos(\theta)))$$

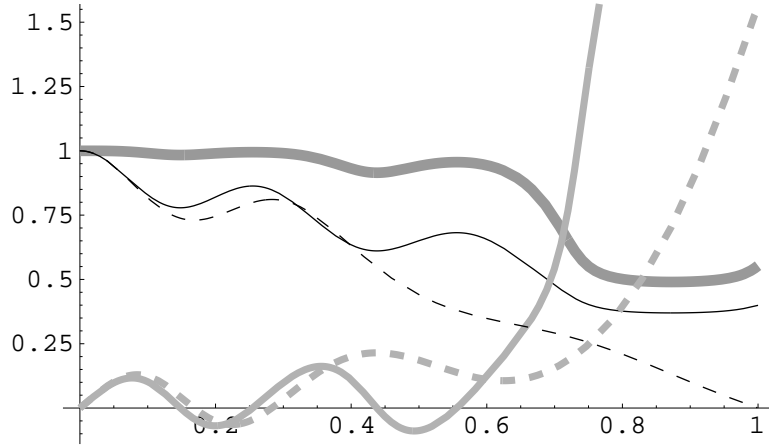


Figure 8: Behavior of solutions to approximations as a function of $\lambda = h/j$, with the same phase parameters used in Fig. 3. Solid curves are from Eq. 14 and dashed from Eq. 12. The black curves are $r = |X|$ (solid) and $|Z|$ (dashed) while the light gray curves are the arguments of X (i.e., θ) and Z . The thick dark gray curve is Y .

$$\begin{aligned} G &= \exp(\nu k \mu ((1 + r^2) \cos(\theta) - 2r)) \\ B &= \nu k \mu (-1 + r^2) \sin(\theta) \end{aligned}$$

and $\nu = \frac{p}{1-p(1-r^2)}$. The initial conditions are $r(0) = 1$, $\theta(0) = 0$ and $Y(0) = 1$, corresponding to all amplitudes equal. The equations for Y and r are unchanged by adding any multiple of 2π to θ .

5.4 Predicted Behavior Using Amplitude Variation

Fig. 8 shows the solution of Eq. 12 and Eq. 14 for the choice of R and T of Fig. 1. For these parameters Eq. 12 gives $|Z| \rightarrow 0$ predicting good performance. But Eq. 14 has $|X| \equiv r$ remaining positive. For small λ , the variation among amplitudes for states with the same cost is small, so $S_{D,C,C'}^{(h)} \approx A_C^{(h)} A_{C'}^{(h)*}$, corresponding to $X \approx Z$. As λ increases, these quantities differ significantly so the two approximations make quite different predictions for the form of the amplitudes at the end of the trial, i.e., at $\lambda = 1$.

As one quantitative evaluation of the approximation including amplitude variation, we can compare its prediction of the scaling of P_{soln} with that seen in Fig. 3. This approximation has $\langle |\psi_s|^2 \rangle \propto |X|^{2c}$ for states with c conflicts. Thus, assuming this expansion holds not only for dominant c but also extends to $c = 0$, i.e., solutions, the probability for a solution, as described in Eq. 15 of the appendix, is

$$\left(\frac{1-p}{1-p(1-|X|^2)} \right)^m$$

with $p = 2^{-k}$. The solution to Eq. 14 shown in Fig. 8 has $|X| \equiv r = 0.399$ at $\lambda = 1$, giving $\langle P_{\text{soln}} \rangle \sim \exp(-0.0957n)$ since $m = 4.25n$, and thus estimates the cost $j/\langle P_{\text{soln}} \rangle$ growing as $\exp(0.0957n)$, very close to the observed growth of $e^{0.10n}$ in Fig. 3. Note the latter quantity is based on median costs of soluble problems while the theory is an estimate of $j/\langle P_{\text{soln}} \rangle$ for all problems.

Fig. 8 shows the contribution from the spread remains small, i.e., Y is near 1, for most of the steps, and then decreases. This corresponds to empirical observations of the behavior of the

algorithm where amplitudes for states near the dominant cost have relatively little variation until the last few steps [27], as illustrated in Fig. 1. Thus Eq. 14 provides an account of this behavior.

These observations show the relations among groups of four assignments in random SAT problems, used to derive Eq. 14, give a fuller account of the algorithm behavior than the simpler theory of the average amplitudes. It does not, however, account for all behaviors. For example, as shown in Fig. 2, continuing the trial beyond step j , i.e., for $\lambda > 1$, gives small oscillations in P_{soln} up to a bit below $\lambda = 2$ followed by a drop to $P_{\text{soln}} \approx 0$. On the other hand, continuing the solution of Eq. 14 beyond $\lambda = 1$ gives small oscillations in r even beyond $\lambda = 3$. That is, Eq. 14 fails to account for the drop in P_{soln} beyond $\lambda \approx 2$ for these parameters. Examining the amplitudes shows they develop multiple peaks so there is no longer a single small range of dominant costs as assumed in deriving Eq. 14 from Eq. 13. Nevertheless, Eq. 14 appears reasonable for describing the behavior over the range of most value for finding solutions, i.e., the range over which the bulk of the amplitude concentrates in low-cost states.

Of particular interest is whether this approximation can also suggest improvements to the algorithm, i.e., the choices of the functions $R(\lambda)$ and $T(\lambda)$. As illustrated in Fig. 8, the solutions to Eq. 14 take on finite nonzero values after the final step, at $\lambda = 1$, for most choices of the phase functions. However, there are special cases in which $r(1) = 0$.

To see what this requires, note that r_λ in Eq. 14 is proportional to Y . Thus for r to decrease to zero, it is important to prevent Y from also becoming small too rapidly. Examining the right-hand sides of Eq. 14 shows Y decreases much more rapidly than r , when r is small, unless θ is near π . Thus one way to have $r(1) = 0$ is for $\theta \rightarrow \pi$ while Y remains bounded above zero. In this case, the $1/r$ term contributing to θ_λ in Eq. 14 becomes large. Thus if θ is to approach π smoothly, the phase adjustment $R(\lambda)$ must also be large near $\lambda = 1$. In particular, the linear form of Eq. 7 near $\lambda = 1$ is not sufficient to allow $r \rightarrow 0$.

Solutions of Eq. 14 with $r(1) = 0$ will not, in general, also satisfy the initial conditions $r(0) = 1$, $\theta(0) = 0$ and $Y(0) = 1$. Nevertheless, appropriate choices of the phase parameter functions, $R(\lambda)$ and $T(\lambda)$, satisfy both sets of conditions. These choices can be found numerically using parameterized forms for these functions and adjusting the parameters to match the required conditions. In these cases $r(\lambda) = \Theta(1 - \lambda)$ near $\lambda = 1$. So for finite n , when $\lambda = 1 - O(1/j)$, i.e., the last few steps, we have $r = O(1/j)$. Thus this approximate analysis indicates $j/\langle P_{\text{soln}} \rangle$ is polynomial in n , hence predicting high performance is possible when the number of steps is much greater than \sqrt{n} .

The choices for the phase parameters are not unique. The additional flexibility may be useful to minimize the variation in performance among different problem instances in the ensemble. More significantly, the need for large phase adjustments for the last few steps to have $r \rightarrow 0$ suggests the asymptotic character of the algorithm may change in the last steps of a trial. In particular, the large adjustments may mean the differential equations of Eq. 14 are no longer good approximations for the discrete map Eq. 13, thereby requiring a more detailed asymptotic analysis for the behavior in the last few steps. In particular, this observation highlights two distinct approximations: first replacing Eq. 8 by Eq. 13 and then estimating its asymptotic behavior by a system of differential equations in Eq. 14. The latter approximation depends on relatively small changes from one step to the next [51] which no longer holds when using large phase parameters.

Empirically, using the large R values near $\lambda = 1$ required by this analysis gives small values for P_{soln} for the small problems feasible to simulate when $j \approx n$. However, when the number of steps j is taken quite large, e.g., $j \approx 100$ for $n = 14$, large R values for the last few steps do give large P_{soln} , but then the cost j/P_{soln} is large due to the large number of steps. Thus a good test of this theory's predictions is beyond the range of feasible simulation.

Nevertheless, the analysis indicates a change in behavior for the last few steps so we consider separate choices for ρ_h and τ_h for the last few steps. That is, we numerically optimize the values

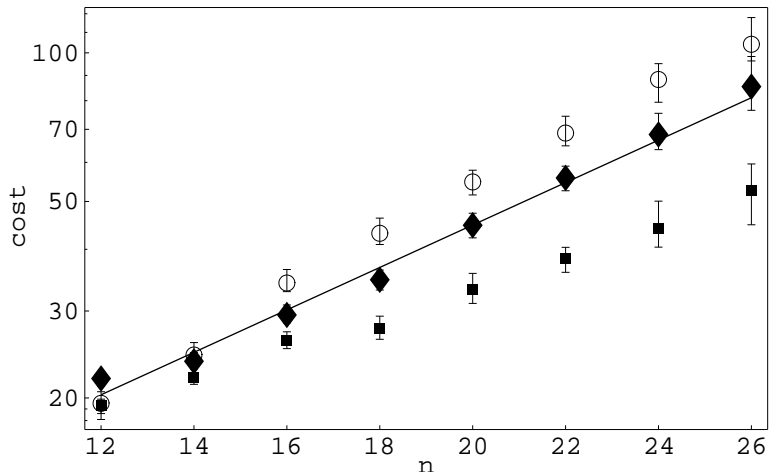


Figure 9: Search cost scaling with the number of steps and phase parameters for the last two steps adjusted to improve performance (square). For comparison, the plot includes the original heuristic (diamond) and GSAT (circle) values from Fig. 3. For each n , all search methods use the same problem instances.

separately for the last few steps while continuing to use the linear variation of Eq. 5 for the remaining steps. For example, Fig. 9 shows the performance using separate values for the last two steps and reducing j/n to minimize median cost as suggested by Fig. 4. The figure shows improved performance with these adjustments, i.e., using a slower growth of j , e.g., $j = \Theta(n^{0.2})$, and different phase adjustments for the last two steps. An exponential fit to the new values gives the median cost growing as $e^{0.08n}$, a somewhat smaller growth rate than the original heuristic.

Because the numerical optimization requires solving a sample of problems multiple times, finding good values for ρ and τ is only possible with small samples, e.g., 50 instances with $n = 16$, 10 with $n = 22$ and 1 with $n = 24$. For $n = 26$, parameter optimization is not feasible so the figure shows the behavior using the parameters found for $n = 24$. Thus the resulting optimal phase values for these small samples are not likely to be the best possible for the ensemble as a whole. Hence the reduced median costs shown in Fig. 9 are upper bounds on the possible performance of the heuristic for these problem sizes. A more comprehensive evaluation would optimize phase parameters separately for every step and use larger training samples. Such a procedure is only feasible for even smaller problems than shown in the figure. Nevertheless, it appears likely that linear variation in the phase parameters is quite good for all but the last few steps.

6 Discussion

As we have seen, search state properties are readily incorporated in quantum search algorithms through amplitude phase adjustments. Properly selected, such adjustments achieve lower overall cost than unstructured search, and require less coherence time for the quantum operations. On the other hand, the additional complexity of such algorithms precludes a simple analytic expression of their average cost and hence makes it difficult to identify those phase choices giving the minimum cost. Nevertheless, approximate techniques provide reasonably good choices and indicate the possibility of polynomial search cost, on average, for hard random k -SAT. The approximations also explain

qualitative features of the algorithm behavior such as the gradual shift in amplitudes toward low-cost states and the increasing amplitude variance in the last few steps of a trial. Moreover, it appears possible to achieve good average performance with phase parameters depending only on the ensemble parameters n , k and m , rather than values tuned to each problem instance.

The averaging procedure is useful because the quantum algorithm evaluates the entire search space and hence incorporates information from all states. By contrast any single run of a classical heuristic samples only a relatively few states which are unlikely to be typical of the search space as a whole, hence precluding theoretical analyses based on average state properties. Thus while quantum heuristics are difficult to evaluate empirically due to the exponential cost of their simulation on classical machines, they could allow a simpler, though still approximate, theoretical analysis than is possible for classical heuristics.

A number of extensions are possible. First, the amplitude shift of Fig. 1 means even if a solution is not found after a trial, the measured state likely has relatively low cost. Thus, like local classical search methods such as GSAT but unlike amplitude amplification, the algorithm applies directly to combinatorial optimization, i.e., finding a minimal conflict state [17]. For example, the shift in amplitudes toward low-cost states is seen in satisfiability problems with no solutions and the traveling-salesman problem [31].

Second, the mean-field analysis also applies to other classes of search problems, provided the probabilities relating problem properties can be determined. This is possible for a variety of commonly studied search ensembles such as coloring random graphs. Ensembles of real-world problems lack analytically known probability distributions, but sampling representative instances allows estimating $P(c|c', d)$. Such estimates may even be useful for analytically simple ensembles, allowing some tuning of phase parameters for a particular problem instance. Conversely, which problem classes have so little correlation among search state properties that quantum algorithms are unlikely to be particularly useful, on average? Such classes may be useful for cryptographic applications [38].

Analysis of problem structure can also indicate how the cost varies through the search space in giving local minima, plateaus, etc. [29, 16]. Such information may help evaluate other types of quantum algorithms that rely on properties of the cost function throughout the space, such as those using partial assignments [6, 25]. As another example, a continuous evolution approach [14] depends on the nature of the eigenvalue spectrum of Hamiltonians encoding the problem costs and hence may benefit from an ensemble analysis of problem structure.

Third, in common with amplitude amplification [3] and some classical methods [39], the growth of $p^{(h)}(0)$, as seen in Fig. 1, means stopping a bit before the largest probability reduces the expected cost. More generally, a mixture or “portfolio” of trials with somewhat different parameter values could give improved trade-offs between expected costs and the variation in costs seen among different instances [32, 20].

Fourth, the heuristic can readily incorporate other computationally-efficient properties of the search states as additional arguments to the phase function ρ . One such a property is how the number of conflicts in a state compares to those of its neighbors, which is used by a number of conventional heuristics including GSAT. Moreover, in analogy with quadratically improving conventional heuristics with amplitude amplification [4], we could also evaluate a conventional heuristic, such as GSAT, for a fixed number of steps and use the cost of the resulting state to adjust phases (either instead of or in addition to the cost of the original state). In this case we would be searching not for a solution state directly but rather for a “good” initial state, i.e., one from which the conventional heuristic rapidly finds a solution. In fact, using just a few steps of GSAT with random SAT instances with $n = 12$ and 20 shows the same shift toward low-cost states as seen in Fig. 1, and the resulting P_{soln} is larger. However, for these problem sizes, the P_{soln} values in the original algorithm are sufficiently large that even if using a few steps of GSAT were able to increase P_{soln} to equal 1, it

would not reduce the overall trial cost due to the additional steps involved in evaluating GSAT. Nevertheless, this approach may be useful for larger problem sizes and illustrates the potential trade-off between the cost of the procedure evaluating search state properties and the resulting probability for a solution, which determines the expected number of trials. In summary, introducing additional properties in the phase adjustment may give better performance, but increases the possible number of distinct parameter values. Thus numerical optimization of parameter values is likely to be more difficult.

An interesting open question is whether this heuristic can benefit from using different parameters and numbers of steps for each trial, as used for amplitude amplification when the number of solutions is not known. As with amplitude amplification, the simulations indicate a wide range of performance among different instances with the same n and m , even if they have the same number of solutions. This approach would rely on the variation among problem instances, not addressed by ensemble averages. Furthermore, the series of low-cost states returned by the unsuccessful trial may also be useful indications of problem structure. This provides another contrast with amplitude amplification where unsuccessful trials simply return randomly selected nonsolution states, with no bias toward lower costs.

While this discussion is encouraging, we should note its limitations. The theory does not provide rigorous bounds on the average search cost. Moreover, even if the algorithm performs well on average, it has no guarantee for specific instances. Nevertheless, restricting consideration to algorithms whose behavior is analytically simple underestimates the potential of quantum computers for typical searches, just as is the case for conventional search algorithms. With ongoing developments in error correction [46, 37] and implementation [10, 9, 34, 43, 41, 1, 35], quantum machines with even a modest number of bits and limited coherence time could help address these issues by evaluating heuristics beyond the range of classical simulation. This will be particularly useful for more complicated heuristics, using additional problem properties, whose theoretical analysis is likely to be more difficult. Exploring their behavior will identify opportunities quantum computers have for using information available in combinatorial searches to significantly improve performance.

Acknowledgments

I thank Scott Kirkpatrick for providing the data on the scaling of the fraction of soluble random 3-SAT problems above the transition point presented in Ref. [44].

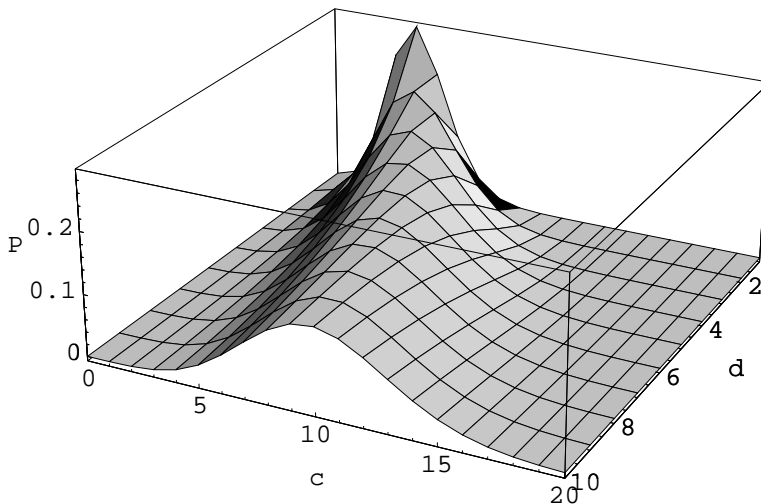


Figure 10: Behavior of $P(c|C, d)$ for $n = 20$, $k = 3$, $m = 80$ and $C = 3$. The values for $d = 0$ are not included: $P(c|C, 0)$ is one when $c = C$ and zero otherwise.

A Derivation of Behavior of S

This appendix describes the derivation of the equation for the behavior of the spread.

A.1 Problem Structure

The algorithm adjusts phases based on the cost associated with each state, and mixes amplitudes based on Hamming distance between pairs of states. Evaluating Eq. 13 requires the relation between distance and difference in cost. For random k -SAT, the required probability distributions are based on multinomial distributions, which are approximately gaussian for large problems.

The probability an assignment has cost C is $P(C) = \binom{m}{C} p^C (1-p)^{m-C}$ where $p = 2^{-k}$ is the probability a single clause conflicts with a given assignment. The expected number of states with cost C is $v(C) = 2^n P(C)$. As one application, if the amplitudes after step h satisfy $|\psi_s|^2 \propto a^{c(s)}$ for some constant a , then the probability to obtain a state with c conflicts $p^{(h)}(c)$ is proportional to $P(c)a^c$ giving

$$p^{(h)}(c) = \frac{P(c)a^c}{(1 - p(1-a))^m} \quad (15)$$

In particular, $p^{(h)}(0)$ is the probability to obtain a solution.

Similarly, the probability two states separated by distance d have costs C and c , respectively, is given by a sum of multinomials depending on the number of clauses conflicting with both states [27]. The corresponding conditional probability $P(c|C, d)$ is peaked for c values close to C when $d \ll n$, as illustrated in Fig. 10. As n increases, the relative width of the probability distribution decreases as $1/\sqrt{n}$, leading to a high correlation between cost and distance for nearby states. The expected number of states with c conflicts at distance d from a state with C conflicts, $v_d(C, c)$, is $\binom{n}{d} P(c|C, d)$.

The quantity $v_{D,d,d',\delta}(C, C', c, c')$ is the sum, over all groups of four states r, r', s, s' with the specified distance relations, of the probability $P(C, C', c, c'|r, r', s, s')$ those states have, respectively,

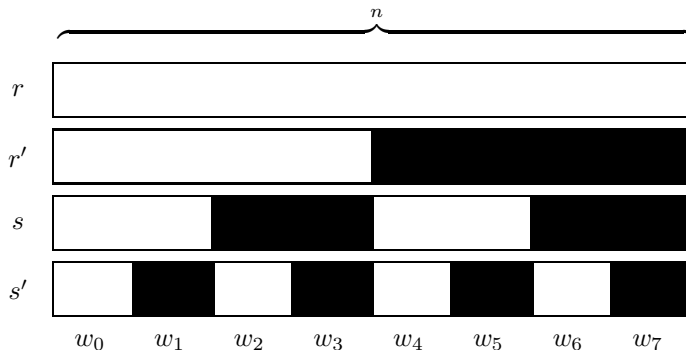


Figure 11: Grouping of variables based on assigned values in assignments r , r' , s and s' , each shown as a horizontal box schematically indicating values assigned to each of the n variables. In each assignment, the value given in r to a variable is shown as white and the opposite value as black. In this diagram, variables are grouped according to the differences in values they are given in the four assignments. For instance, the first group, consisting of w_0 variables, has those variables assigned the same value in all four assignments. The fourth group, with w_3 variables, has those variables with the same values in r and r' , but opposite values in s and s' .

costs C, C', c, c' . For random k -SAT, this probability depends only on the way these states share variables with the same assigned values, specified by $W = \{w_0, w_1, \dots, w_7\}$ and illustrated in Fig. 11. For example, w_0 counts the number of variables assigned the same value in all four states. These possibilities completely specify the distances between the states, namely,

$$\begin{aligned}
 D = d(r, r') &= w_4 + w_5 + w_6 + w_7 \\
 d = d(r, s) &= w_2 + w_3 + w_6 + w_7 \\
 d' = d(r', s') &= w_1 + w_3 + w_4 + w_6 \\
 \delta = d(s, s') &= w_1 + w_2 + w_5 + w_6
 \end{aligned} \tag{16}$$

For a given set of values W , there are $N(W) = 2^n \binom{n}{w_0, \dots, w_7}$ corresponding choices for the four states.

Generalizing the case for two states, the probability $P(C, C', c, c'|W)$ is a multinomial sum over the ways the clauses can be selected to conflict with different subsets of the states, constrained to give the specified number of conflicts to each of the states. These clause selections are determined by the principle of inclusion and exclusion [42]. Finally, $v_{D,d,d',\delta}(C, C', c, c')$ is the sum of $N(W)P(C, C', c, c'|W)$ over those choices of W matching the specified distances between the states.

Because of the constraints on the conflicts and distances, the resulting 4-state probability does not have a simple closed form. It is nevertheless readily calculated and, for large problems, is approximately a normal distribution. For use in the expansion described in the next section, this distribution is multiplied by powers and summed, which can be done directly using the multinomial theorem.

A.2 Expansion for Large Problem Sizes

Eq. 13 simplifies in the limit of large n using the following observations of its structure. First, for weak mixing, i.e., when τ_h is taken to be $O(1/n)$, the u_d values in Eq. 13 decrease as n^{-d} so the main contributions are from terms with $d, d' \ll n$. Second, as illustrated in Fig. 10, nearby states

generally have about the same cost so the c, c' sums in Eq. 13 are dominated by the values close to C, C' , respectively. Finally, from Fig. 7, small values for d, d' also require $\delta \sim D$.

Thus to evaluate Eq. 13, expand $S_{\delta,c,c'}$ as $S_{D,C,C'} Y^{\delta-D} X^{c-C} (X^*)^{c'-C'}$ for values of δ, c, c' close to D and the dominant C, C' . We are particularly interested in the behavior for D near zero.

With this expansion, the sum over c, c' in Eq. 13 is sum of a multinomial multiplied by powers, which is readily evaluated for given distance relations W in terms of the fraction of clauses conflicting with various subsets of the four states.

For the sums over d, d' , the restrictions $d, d' \ll n$ mean the variable groups shown in Fig. 7 are all much less than n except possibly for the two groups contributing to neither the value of d nor d' . From Eq. 16 these are $w_0 = n - D - w_1 - w_2 - w_3$ and $w_5 = D - w_4 - w_6 - w_7$. This observation, combined with the contributions from the u_d factors in Eq. 13, allow the d, d' sums to be approximated as exponentials.

For evaluating the probability in states with cost C at step h we need only $S_{0,C,C}^{(h)}$ whose value and change from one step to the next is determined by the behavior for $D \ll n$ and hence C' close to C . Furthermore, the bulk of the probability is concentrated in states with a narrow range of costs. Thus we can focus on the behavior near the dominant C value at each step.

Let $X = r e^{i\theta}$ with r and θ real-valued. With a narrow distribution of costs, the dominant C equals the average, i.e., $\sum_C CP(C)S(0, C, C) \propto \sum_C CP(C)r^{2C}$. Thus the dominant C equals [27] $r^2 \nu m$ where $\nu = \frac{p}{1-p(1-r^2)}$. Hard random k -SAT problems have $m \propto n$, so significant amplitude is in low-cost states whenever r is of order $1/\sqrt{n}$. When $r \ll 1/\sqrt{n}$, the lowest cost states (i.e., the solutions if the problem instance is soluble) have most of the amplitude.

Expanding around the dominant C value then produces Eq. 14.

References

- [1] M. Bayer et al. Coupling and entangling of quantum states in quantum dot molecules. *Science*, 291:451–453, 2001.
- [2] Charles H. Bennett, Ethan Bernstein, Gilles Brassard, and Umesh V. Vazirani. Strengths and weaknesses of quantum computing. *SIAM Journal on Computing*, 26:1510–1523, 1997.
- [3] Michel Boyer, Gilles Brassard, Peter Hoyer, and Alain Tapp. Tight bounds on quantum searching. In T. Toffoli et al., editors, *Proc. of the Workshop on Physics and Computation (PhysComp96)*, pages 36–43, Cambridge, MA, 1996. New England Complex Systems Institute.
- [4] Gilles Brassard, Peter Hoyer, and Alain Tapp. Quantum counting. In K. Larsen, editor, *Proc. of 25th Intl. Colloquium on Automata, Languages, and Programming (ICALP98)*, pages 820–831, Berlin, 1998. Springer. Los Alamos preprint quant-ph/9805082.
- [5] N. J. Cerf and S. E. Koonin. Monte Carlo simulation of quantum computation. In *Proc. of IMACS Conf. on Monte Carlo Methods*, 1997. Los Alamos preprint quant-ph/9703050.
- [6] Nicolas J. Cerf, Lov K. Grover, and Colin P. Williams. Nested quantum search and NP-complete problems. In *Applicable Algebra in Engineering, Communication and Computing*. Springer, Berlin, 1998. Los Alamos preprint quant-ph/9806078.
- [7] Peter Cheeseman, Bob Kanefsky, and William M. Taylor. Where the really hard problems are. In J. Mylopoulos and R. Reiter, editors, *Proceedings of IJCAI91*, pages 331–337, San Mateo, CA, 1991. Morgan Kaufmann.

- [8] I. L. Chuang, R. Laflamme, P. W. Shor, and W. H. Zurek. Quantum computers, factoring and decoherence. *Science*, 270:1633–1635, 1995.
- [9] Isaac L. Chuang, Neil Gershenfeld, and Mark Kubinec. Experimental implementation of fast quantum searching. *Physical Review Letters*, 80:3408–3411, 1998.
- [10] Isaac L. Chuang, Lieven M. K. Vandersypen, Xinlan Zhou, Debbie W. Leung, and Seth Lloyd. Experimental realization of a quantum algorithm. *Nature*, 393:143–146, 1998. Los Alamos preprint quant-ph/9801037.
- [11] D. Deutsch. Quantum theory, the Church-Turing principle and the universal quantum computer. *Proc. R. Soc. London A*, 400:97–117, 1985.
- [12] David P. DiVincenzo. Quantum computation. *Science*, 270:255–261, 1995.
- [13] Stefan Edelkamp and Richard E. Korf. The branching factor of regular search spaces. In *Proc. of the 15th Natl. Conf. on Artificial Intelligence (AAAI98)*, pages 299–304, Menlo Park, CA, 1998. AAAI Press.
- [14] Edward Farhi, Jeffrey Goldstone, Sam Gutmann, and Michael Sipser. Quantum computation by adiabatic evolution. Technical Report MIT-CTP-2936, MIT, Jan. 2000.
- [15] Richard P. Feynman. *Feynman Lectures on Computation*. Addison-Wesley, Reading, MA, 1996.
- [16] J. Frank, P. Cheeseman, and J. Stutz. When gravity fails: Local search topology. *J. of Artificial Intelligence Research*, 7:249–281, 1997.
- [17] Eugene C. Freuder and Richard J. Wallace. Partial constraint satisfaction. *Artificial Intelligence*, 58:21–70, 1992.
- [18] M. R. Garey and D. S. Johnson. *Computers and Intractability: A Guide to the Theory of NP-Completeness*. W. H. Freeman, San Francisco, 1979.
- [19] Ian P. Gent, Ewan MacIntyre, Patrick Prosser, and Toby Walsh. The constrainedness of search. In *Proc. of the 13th Natl. Conf. on Artificial Intelligence (AAAI96)*, pages 246–252, Menlo Park, CA, 1996. AAAI Press.
- [20] C. P. Gomes and B. Selman. Algorithm portfolio design: Theory vs. practice. In D. Geiger and P. Shenoy, editors, *Proc. of the 13th Conf. on Uncertainty in AI (UAI-97)*, pages 190–197, Los Altos, CA, 1997. Morgan Kaufmann.
- [21] Ronald Graham, Oren Patashnik, and Donald E. Knuth. *Concrete Mathematics: A Foundation for Computer Science*. Addison-Wesley, Reading, MA, 2nd edition, 1994.
- [22] Lov K. Grover. Quantum mechanics helps in searching for a needle in a haystack. *Physical Review Letters*, 78:325–328, 1997. Los Alamos preprint quant-ph/9706033.
- [23] Lov K. Grover. Quantum search on structured problems. *Chaos, Solitons, and Fractals*, 10:1695–1705, 1999.
- [24] Tad Hogg. Exploiting problem structure as a search heuristic. *Intl. J. of Modern Physics C*, 9:13–29, 1998.

- [25] Tad Hogg. A framework for structured quantum search. *Physica D*, 120:102–116, 1998. Los Alamos preprint quant-ph/9701013.
- [26] Tad Hogg. Highly structured searches with quantum computers. *Physical Review Letters*, 80:2473–2476, 1998. Preprint at publish.aps.org/eprint/gateway/eplist/aps1997oct30_002.
- [27] Tad Hogg. Quantum search heuristics. *Physical Review A*, 61:052311, 2000. Preprint at publish.aps.org/eprint/gateway/eplist/aps1999oct19_002.
- [28] Tad Hogg. Single-step quantum search using problem structure. *Intl. J. of Modern Physics C*, 11:739–773, 2000. Los Alamos preprint quant-ph/9812049.
- [29] Tad Hogg, Bernardo A. Huberman, and Colin P. Williams, editors. *Frontiers in Problem Solving: Phase Transitions and Complexity*, volume 81, Amsterdam, 1996. Elsevier. Special issue of *Artificial Intelligence*.
- [30] Tad Hogg, Carlos Mochon, Eleanor Rieffel, and Wolfgang Polak. Tools for quantum algorithms. *Intl. J. of Modern Physics C*, 10:1347–1361, 1999. Los Alamos preprint quant-ph/9811073.
- [31] Tad Hogg and Dmitriy Portnov. Quantum optimization. *Information Sciences*, 128:181–197, 2000. Los Alamos preprint quant-ph/0006090.
- [32] Bernardo A. Huberman, Rajan M. Lukose, and Tad Hogg. An economics approach to hard computational problems. *Science*, 275:51–54, 1997.
- [33] Anil Kamath, Rajeev Motwani, Krishna Palem, and Paul Spirakis. Tail bounds for occupancy and the satisfiability threshold conjecture. In S. Goldwasser, editor, *Proc. of 35th Symposium on Foundations of Computer Science*, pages 592–603. IEEE Press, 1994.
- [34] Bruce E. Kane. A silicon-based nuclear spin quantum computer. *Nature*, 393:133, 1998.
- [35] D. Kielpinski et al. A decoherence-free quantum memory using trapped ions. *Science*, 291:1013–1015, 2001.
- [36] Scott Kirkpatrick and Bart Selman. Critical behavior in the satisfiability of random boolean expressions. *Science*, 264:1297–1301, 1994.
- [37] Emanuel Knill, Raymond Laflamme, and Wojciech H. Zurek. Resilient quantum computation. *Science*, 279:342–345, 1998.
- [38] Neal Koblitz. *Algebraic Aspects of Cryptography*. Springer, Berlin, 1998.
- [39] Michael Luby, Alistair Sinclair, and David Zuckerman. Optimal speedup of Las Vegas algorithms. Technical Report TR-93-010, Intl. Comp. Sci. Inst., Berkeley, CA, March 1993.
- [40] Alan Mackworth. Constraint satisfaction. In S. Shapiro, editor, *Encyclopedia of Artificial Intelligence*, pages 285–293. Wiley, NY, 1992.
- [41] J. E. Mooij et al. Josephson persistent-current qubit. *Science*, 285:1036–1039, 1999.
- [42] E. M. Palmer. *Graphical Evolution: An Introduction to the Theory of Random Graphs*. Wiley Interscience, NY, 1985.
- [43] P. M. Platzman and M. I. Dykman. Quantum computing with electrons floating on liquid helium. *Science*, 284:1967–1969, 1999.

- [44] Bart Selman and Scott Kirkpatrick. Critical behavior in the computational cost of satisfiability testing. *Artificial Intelligence*, 81:273–295, 1996.
- [45] Bart Selman, Hector Levesque, and David Mitchell. A new method for solving hard satisfiability problems. In *Proc. of the 10th Natl. Conf. on Artificial Intelligence (AAAI92)*, pages 440–446, Menlo Park, CA, 1992. AAAI Press.
- [46] P. Shor. Scheme for reducing decoherence in quantum computer memory. *Physical Review A*, 52:2493–2496, 1995.
- [47] Peter W. Shor. Algorithms for quantum computation: Discrete logarithms and factoring. In S. Goldwasser, editor, *Proc. of the 35th Symposium on Foundations of Computer Science*, pages 124–134, Los Alamitos, CA, November 1994. IEEE Press.
- [48] George W. Snedecor and William G. Cochran. *Statistical Methods*. Iowa State Univ. Press, Ames, Iowa, 6th edition, 1967.
- [49] Lee Spector, Howard Barnum, Herbert J. Bernstein, and Nikhil Swamy. Finding a better-than-classical quantum AND/OR algorithm using genetic programming. In P. Angeline, editor, *Proc. of the 1999 Congress on Evolutionary Computing*, Washington, DC, 1999. IEEE.
- [50] Andrew Steane. Quantum computing. *Reports on Progress in Physics*, 61:117–173, 1998.
- [51] Nicholas C. Wormald. Differential equations for random processes and random graphs. *Annals of Applied Probability*, 5:1217–1235, 1995.